International Journal of Applied Earth Observation and Geoinformation 125 (2023) 103539

Contents lists available at ScienceDirect

International Journal of Applied Earth Observation and Geoinformation

journal homepage: www.elsevier.com/locate/jag

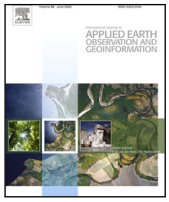

Assessing spatiotemporal bikeability using multi-source geospatial big data: A case study of Xiamen, China

Shaoqing Dai [a,h], Wufan Zhao [a,b,*], Yanwen Wang [a], Xiao Huang [c], Zhidong Chen [d], Jinghan Lei [d], Alfred Stein [a], Peng Jia [e,f,g,h]

[a] Faculty of Geo-Information Science and Earth Observation (ITC), University of Twente, 7514AE Enschede, The Netherlands
[b] Geomatics Section, Department of Civil Engineering, Faculty of Engineering Technology, KU Leuven, 9000 Gent, Belgium
[c] Department of Geosciences, University of Arkansas, Fayetteville, AR 72701, United States of America
[d] Xiamen Urban Planning and Design Institute, China
[e] School of Resource and Environmental Sciences, Wuhan University, Wuhan, China
[f] Hubei Luojia Laboratory, Wuhan, China
[g] School of Public Health, Wuhan University, Wuhan, China
[h] International Institute of Spatial Lifecourse Health (ISLE), Wuhan University, Wuhan, China

ARTICLE INFO

Keywords:
Bike-sharing
Bikeability
Built environment
Multi-source data
Spatialtemporal

ABSTRACT

This study focuses on the development of a new framework for evaluating bikeability in urban environments with the aim of enhancing sustainable urban transportation planning. To close the research gap that previous studies have disregarded the dynamic environmental factors and trajectory data, we propose a framework that comprises four sub-indices: safety, comfort, accessibility, and vitality. Utilizing open-source data, advanced deep neural networks, and GIS spatial analysis, the framework eliminates subjective evaluations and is more efficient and comprehensive than prior methods. The experimental results on Xiamen, China, demonstrate the effectiveness of the framework in identifying areas for improvement and enhancing cycling mobility. The proposed framework provides a structured approach for evaluating bikeability in different geographical contexts, making reproducing bikeability indices easier and more comprehensive to policymakers, transportation planners, and environmental decision-makers.

1. Introduction

The urban mobility landscape is undergoing significant changes as cities strive for a more sustainable future (Eren and Uz, 2020; Steinacker et al., 2022). Active modes of transportation, including walking, cycling, and public transit, offer numerous environmental, health, and economic advantages compared to the use of private vehicles (Ito and Biljecki, 2021; Gan et al., 2021; Wang et al., 2022). Cycling, in particular, has gained widespread support as one of the most sustainable, eco-friendly, and healthy modes of urban transportation (Huang et al., 2021, 2022b). Its positive attributes influence individuals' travel behaviors, encouraging a shift towards active travel modes. The introduction of bicycle-sharing systems has resulted in a substantial increase in bicycle trips, rising from 5.5% to 11.6% among 36 cities in China (Long and Zhao, 2020). Investigating a framework for evaluating the bike-friendliness of cities is crucial for enhancing urban functionality and advancing sustainable transportation planning.

The scientific community has shown increasing interest in evaluating the level of support for walking and biking, referred to as 'walkability' and 'bikeability', in communities (Pan et al., 2021; Yang et al., 2021). The factors that drive bikeability in cities, such as environmental consciousness, functional aspects like convenience and time management, the need for exercise, or affordability, have been extensively researched. Despite this, there is still no universally accepted definition of "bikeability" (Hagen and Rynning, 2021). On one hand, bikeability is seen as a gauge of a city's bicycle network's comfort, accessibility, and convenience, used for comparing cities (Lowry et al., 2012). On the other hand, it can be defined as the extent to which the built environment promotes safe cycling and is conducive to it (Kellstedt et al., 2021), with more emphasis on the suitability of a particular location for cycling. In this study, we concentrate on quantifying the suitability of the built environment for bicycling by considering both the factors that influence choosing the bicycle as a mode of transportation and environmental factors. Bikeability is defined as a single composite index that can be used to promote cycling based on multiple perspectives: safety, comfort, accessibility, and vitality.

* Corresponding author at: Faculty of Geo-Information Science and Earth Observation (ITC), University of Twente, 7514AE Enschede, The Netherlands.
E-mail address: wufan.zhao@kuleuven.be (W. Zhao).

https://doi.org/10.1016/j.jag.2023.103539
Received 10 March 2023; Received in revised form 21 October 2023; Accepted 22 October 2023

The concept of the bikeability index has been extensively studied using a range of indices from single to multiple sub-indices and utilizing both questionnaires to quantitative evaluations based on multi-source data (Chen et al., 2022; Codina et al., 2022). These studies are essential for identifying areas for improvement and for demonstrating the need for change to politicians and the public. Traditional questionnaire-based evaluations use basic statistical models to produce subjective evaluation indicators (Parkin et al., 2007; Wang et al., 2018; Caigang et al., 2022). However, recent technological advancements, such as computer vision and deep learning (Zhang et al., 2021; Tang et al., 2023), combined with the availability of new data sources like street view imagery and air quality, allow for a more detailed examination of the built environment's impact on mobility assessments. Studies have shown a significant relationship between cycling behavior and various built environment and contextual factors, including bikeway density, bikeway width, bikeway exclusiveness, slopes, and the presence of nearby green spaces (Parkin et al., 2007; Winters et al., 2010; Wang et al., 2018; Hyland et al., 2018; Jia et al., 2021; Jia, 2021). However, cycling is greatly influenced by dynamic environmental factors such as weather and time of day, making the measurement of bikeability a complex and spatially specific challenge that requires further attention. Previous research has focused mainly on public bike systems with fixed rental points, which restricts the freedom of cycling activities for residents and limits the accuracy of origin–destination spatial distribution and cyclist path characteristics (Huang et al., 2022a). Additionally, the relative newness of bike-sharing data and the lack of tools for measuring the built environment at a fine granularity make it challenging to perform large-scale investigations on spatial–temporal analysis and validation of cycling route selection preferences (Zhang et al., 2019; Dai et al., 2020).

Various studies have explored the factors influencing cycling behaviors and have developed a range of indicators to assess the bicycle-friendly environment from various perspectives (Nielsen and Skov-Petersen, 2018; Porter et al., 2020). Traditionally, indicators such as speed, commercial facility density, and bus stop availability have been used to measure accessibility and promote bikeability in cities (Hankey et al., 2017; Eren and Uz, 2020). Additionally, weather conditions, like wind speed, precipitation, and temperature, have been associated with cycling safety and comfort (Eren and Uz, 2020). Recently, visual elements such as sky and green spaces, analyzed through computer vision techniques, have been applied in cycling assessments (Ito and Biljecki, 2021). Despite these efforts, bikeability has often overlooked personal exposure to air pollution during cycling, there is the mounting evidence that links air pollution to negative health outcomes, including cardiovascular and respiratory diseases, as well as cancer (Giallouros et al., 2020; Zhao et al., 2018; Tran et al., 2020).

A rationale aim of this study to develop a cutting-edge bikeability evaluation framework that considers dynamic climate, trajectory data, and other important factors. The framework is used to analyze the spatio-temporal dynamics of city-level streets and their impact on bikeability. To validate the findings, we cross-reference the analysis with spatio-temporal hotspot statistics. Utilizing open-source data, such as land use maps, road networks, and Google Street View (GSV) imagery, we employ a combination of spatial statistics, deep neural network (DNN) techniques (Zhu et al., 2022; Zhao et al., 2022, 2023), and Geographic Information System (GIS) (Jia et al., 2017) tools to assess the framework's effectiveness. Xiamen, China, serves as the case study for this research. The ultimate goal is to provide policymakers and experts with a structured framework for evaluating bikeability in different geographical contexts, making the process of replicating bikeability index easier and more comprehensive.

2. Data and study area

2.1. Study area

Xiamen is a bustling coastal city located in Fujian Province, China and is considered a special economic zone of national significance (Fig. 1). With its status as a major port and tourist destination, Xiamen serves as a central hub in the region. The city encompasses six districts and spans an area of 1,700.61 km^2, boasting a population of over 5.28 million as of 2021. Given its extensive bike-sharing trajectory coverage, Xiamen Island was selected as the focal point of this study.

2.2. Data and preprocessing

We made use of various big data sources, including (1) Bike-sharing trajectory data collected during the morning hours of 6:00 to 10:00 a.m. from December 21 to 25th, 2020 (provided by the Digital China Innovation Contest 2021, https://data.xm.gov.cn/contest-series/digit-china-2021). (2) Digital Elevation Model (DEM) data from Geospatial Data Cloud website (http://www.gscloud.cn/). (3) Mobile phone signaling data to estimate population volume (provided by China Unicom). (4) Point of Interest data related to food, life services, interests, and shopping from Baidu Map. (5) Street view imagery from Baidu Map. (6) Air quality monitoring data from the ecology and environment agency for the period of December 21 to 25th. (7) European reanalysis version 5(ERA5) Climate datasets from the European Centre for Medium-Range Weather Forecasts and Copernicus(https://doi.org/10.24381/cds.adbb2d47). All data were collected during the morning hours of 6:00 to 10:00 a.m. from December 21 to 25th, 2020.

In this study, we carried out the pre-processing of multiple sources of spatiotemporal big data. The following measures were taken:

1. Filtering and processing of road segments to determine bikeability. This involved performing a topology check and splitting segments longer than 500 m and shorter than 200 m (resulting in 2,854 segments in total).
2. Collection and analysis of mobile phone signaling data to estimate population density in 250×250 m grids for the specified time period.
3. Processing of bike-sharing trajectory data. This involved filtering trajectories that were within Xiamen Island, at least 1 min long and over 100 m in length. The average speed of each trajectory was calculated as the sum of the displacement between points divided by the time difference between the points. The bike-sharing trajectory was then matched with road segments, and the number of trajectories and average speed were determined for each segment.
4. Collection and processing of air quality station monitoring data and climate data, which were formatted for spatial interpolation.
5. Sampling of points from each road segment generated in step 1, followed by downloading of the corresponding 360° street view imagery.

3. Method

A rationale aim of this study was to understand the factors that impact the behavior of residents' cycling activities using machine learning, deep learning, and trajectory mining algorithms on multi-sources spatiotemporal big data. The data sources utilized include bike-sharing trajectory, DEM, mobile phone signaling data, points of interest (POI), street view imagery, air quality station monitoring data, and ERA5 climate datasets. Using road network segments as the study units, we build an evaluation system for the traffic friendliness of active transport systems and evaluate the bikeability of our target city, i.e., Xiamen.

3.1. Proposed bikeability framework

We construct the bikeability evaluation framework by combining the collected multi-source spatio-temporal big data (Fig. 2). The proposed bikeability evaluation framework contains four subindexes, i.e., safety, comfort, accessibility, and vitality, and thirteen influencing indicators, i.e., wind speed, road slope, precipitation, temperature, sky

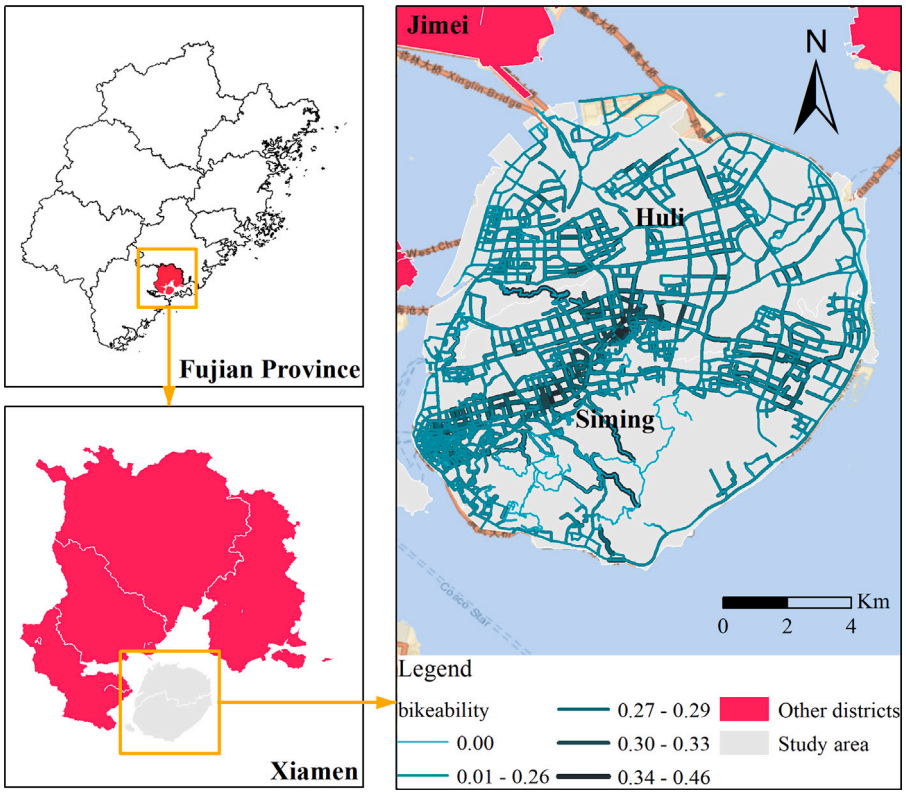

Fig. 1. Study area of Xiamen island.

view index, green view index, trajectory sinuosity, air pollution, average speed of trajectory, public transportation accessibility, commercial accessibility, number of trajectory and crowdedness. All indicators used in our framework belong to objective and quantitative measurements.

Safety is evaluated based on three factors: wind speed, road slope, and precipitation. Strong winds can make riding more challenging, while steep slopes increase the risk of accidents while descending. Precipitation, such as rain or snow, can make the roads slippery and reduce visibility, which in turn affects the safety and comfort of riders.

Comfort is determined by five factors: temperature, sky view index, green view index, sinuosity, and air pollution. High or low temperatures, both during summer and winter, can cause discomfort for riders. The Sky view index and green view index assess a rider's subjective perception of the sky and vegetation they observe during the ride, with a higher ratio resulting in increased comfort. The sinuosity of the cycling route and air pollution, particularly PM2.5, can negatively impact the comfort and health of riders.

Accessibility is evaluated by three factors: average speed of trajectory, public transportation accessibility, and commercial accessibility. A slower average cycling speed can indicate a less friendly route for cyclists, while proximity to public transportation and commercial facilities can increase the convenience of cycling. The number of POIs is used as an indicator of commercial accessibility.

Vitality is focused on the purpose of riding and is determined by two factors: the number of trajectories and crowdedness. A higher number of trajectories and more crowdedness indicate a higher utilization rate of shared bikes and more cyclists on the road, reflecting a more friendly and vibrant cycling environment. The number of mobile phone signals is used as an indicator representing crowdedness.

3.2. Subindexes and bikeability index calculation

- **Safety**: wind speed and precipitation were downscaled to 100 m resolution using the 0.1° ERA reanalysis data via using spatial interpolation. The slope was calculated from the STRM digital elevation model with a 30 m resolution. The spatial interpolation methods applied include thin plate splines (TPS) and Ordinary Kriging (OK). TPS is a 2-D interpolation algorithm that uses longitude, latitude, and climate indices, such as horizontal and vertical wind speed at 10 m and precipitation, to minimize a multivariate function based on a coefficient of relaxation (λ), an integer, and a series of positive weights. OK is a geostatistics method that converts the spatial interpolation into a variance minimization optimization problem and solves for the weights between observed points and target locations.
- **Comfort**: Temperature and air pollution were downscaled to 100 m using a combination of ERA reanalysis data and air pollution monitoring site measurements. Spatial interpolation was used to obtain these values. The sky view index and green view index were calculated from street view imagery using the pre-trained deep learning model Deeplab v3+ (Chen et al., 2018) (Fig. 3). The calculation of sky view factors and green view index, i.e., the ratio of the number of pixels for a specific object to the total number of pixels, follows.

$$BEVI_t = \frac{\text{Area}_{t,x}}{\text{Area}_t} \times 100\% \quad (1)$$

where $BEVI_t$ represents the sky view factors or green view index of street view imagery at the sampling locations ($t = 1, 2, \ldots, n$). $\text{Area}_{t,x}$ represents the number of pixels for the built environmental factors x (x represents green space or sky) of street view imagery at the sampling locations. $Area_t$ represents the total number of pixels of street view imagery at the sampling locations. Sinuosity, defined as the ratio between the actual travel distance and the direct distance, represents the bending degree of the object in the length direction. Our study regards the bike-sharing trajectories as the investigating object. The sinuosity is defined as the ratio of the driving distance and the straight-line distance

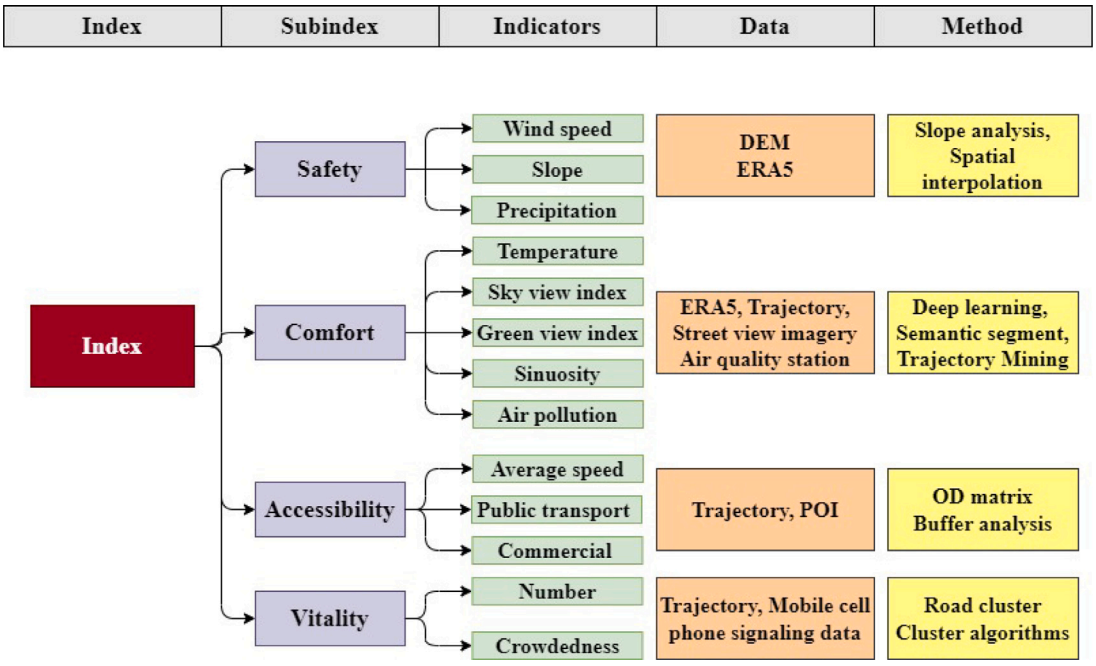

Fig. 2. The proposed bikeability framework.

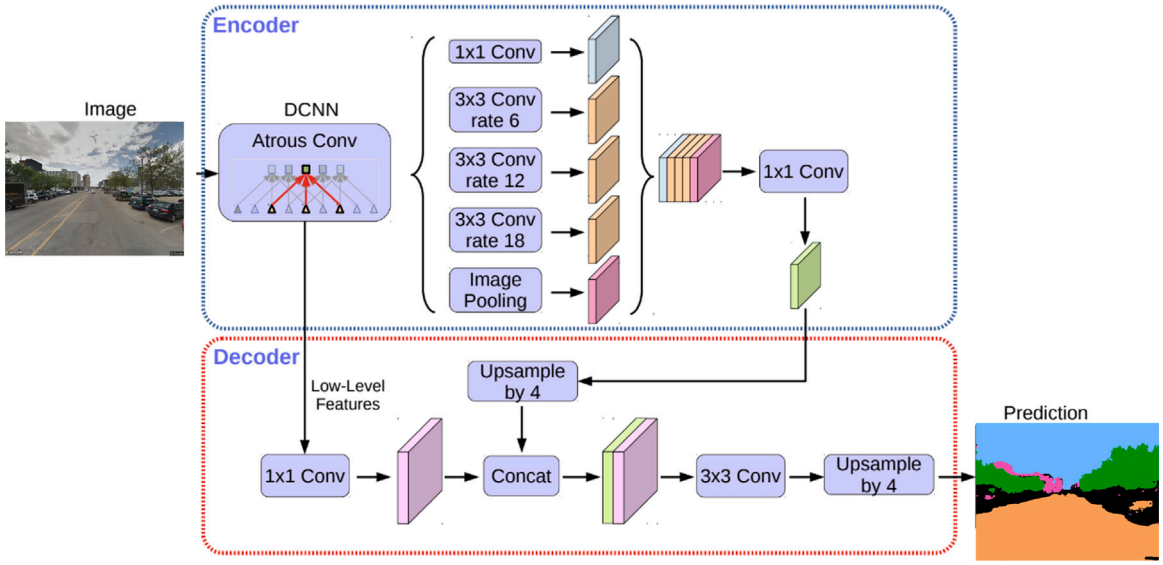

Fig. 3. Street view imagery semantic segmentation process, revised from Chen et al. (2018).

from the origin to the destination:

$$\text{Sinuosity} = \frac{\text{Driving Distance}}{\sqrt{(x_2 - x_1)^2 + (y_2 - y_1)^2}} \quad (2)$$

where, (x_1, y_1) and (x_2, y_2) denote the coordinate of the origin and the destination.

- **Accessibility**: Accessibility is measured using three indicators: average speed of bike trajectories, public transport accessibility, and commercial accessibility. The average speed is calculated as the length of the bike trip divided by its duration. Public transport accessibility is assessed by determining the shortest distance from the mid-point of a road segment to the nearest public transport stop, providing an indication of the convenience of using public transportation for traveling from one place to another. Commercial accessibility is evaluated by counting the density of commercial facilities along the road segments within a 50 m range on both sides. A high number of commercial facilities is vital for keeping an area bustling and thriving. The locations of these commercial facilities are extracted using POI data.
- **Vitality**: Vitality is evaluated based on two factors: the number of bike-sharing trajectories and crowdedness. To determine the number of bike-sharing trajectories, we count the number of bikes used within each road segment. To evaluate crowdedness, we analyze mobile phone signaling data using a non-parametric method of kernel density estimation. This method helps in identifying spatial clusters and hotspots of residential travel activity in a given space.

To measure bikeability, we create a spatiotemporal database that integrates multi-source spatiotemporal big data and road network segments. We combine all of the relevant indicators and assigning weights to each using principal component analysis (PCA) (Wold et al., 1987), a

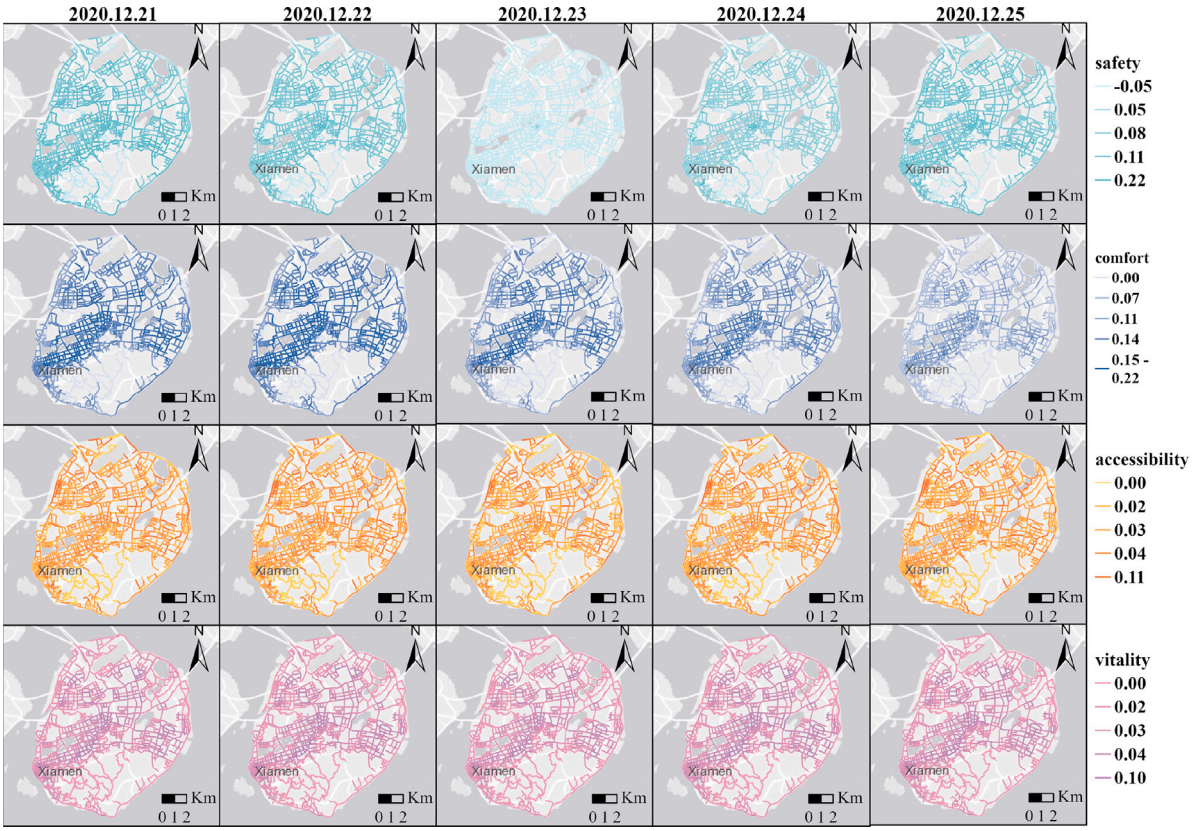

Fig. 4. The figures show the daily safety, comfort, accessibility, and vitality of Xiamen Island from top row to bottom row, where from left column to right column respectively represent the dates from 21 to 25th.

widely used method for data dimensionality reduction. The weighting process of key indicators to form a composite index can be achieved through various methods, like PCA, factor analysis, data envelopment analysis (DEA), benefit of the doubt (BoD), Delphi method, and analytic hierarchy process (AHP). Delphi and AHP rely on expert knowledge and are subjective in nature (Ran et al., 2021). DEA and BoD focus on measuring efficiencies of decision-making units and may emphasize well-performing indicators, but they may not cover the entire evaluation system of bikeability (Lemke and Bastini, 2020). In comparison, PCA is an objective, bottom-up, and data-driven weighted algorithm with a solid mathematical foundation (Yu et al., 2013). It allows for dimensionality reduction of big data, capturing the maximum amount of variance present and generating uncorrelated components. Therefore, we used PCA to evaluate bikeability based on spatial–temporal geospatial big data. The square root of corresponding eigenvalues namely loadings in PCA will be assigned as weighted coefficients, following the works by Bao et al. (2022) and Liu et al. (2022). The number of extracted components is four, and the degree of explained variance reaches 69.6%. The oblique transformation is variance maximum. The formula for the bikeability index follows:

$$\text{Bikeability} = a_1 \cdot x_1 + a_2 \cdot x_2 + \cdots + a_{13} \cdot x_{13} \quad (3)$$

where $a_1, a_2, \ldots, a_{13}$ represent the weight of each indicator generated by PCA. $x_1, x_2, \ldots, x_{13}$ represent the ith normalized indicators ($i = 1, 2, \ldots \ldots, 13$) such as wind speed, slope, ……, crowdedness.

4. Results

4.1. Spatiotemporal analysis of subindexes

We first present and discuss the results of four subindexes across Xiamen Island on a daily basis from December 21 to 25th, 2020 (Fig. 4).

The variability of the safety subindex is demonstrated in Fig. 4 first row, which highlights the changes in safety over time. On the 21st, 22nd, and 25th, the safety values are relatively high at 0.092, 0.081, and 0.084, respectively. However, the safety value on the 23rd decreases significantly to −0.024 due to the rainfall on that day. This shift in weather conditions caused the safety subindex to change from a positive to a negative value. The safety returned to its normal range on the 24th when the rain stopped, resulting in a positive value of 0.061. When examining the spatial aspect, on the non-rainy days (21st, 22nd, and 25th), around 20% of road sections were found to have a safety subindex greater than 0.1 (80% quantile), and these sections remained consistent across different dates (Table 1).

As depicted in the second row of Fig. 4, the comfort subindex exhibits noticeable fluctuations over the course of five days. The values decline gradually from 0.103 on the 21st to 0.085 on the 24th. However, on the 25th, there is a sharp drop to 0.060. A closer examination of the indicators used to compose the comfort subindex reveals that the average concentration of PM2.5 on the 25th exceeded 30 μg m^{-3}, which was much higher compared to the other days. Additionally, the average temperature on the 25th was also the lowest, which further impacted the comfort subindex value.

In contrast to the safety and comfort subindexes, the accessibility subindex showed minimal variations over the five-days study period, as shown in Fig. 4 third row. This is likely due to the study period consisting of working days, which led to consistent commuting conditions for cyclists every day. Two of the key indicators used to compose the accessibility subindex, bus traffic and POI density, remained constant. The only varying indicator, average cycling speed, was primarily influenced by road conditions, such as smoothness and traffic, rather than time. For instance, roads that were smooth and had less traffic generally had higher average cycling speeds, regardless of the day of the week. As a result, the values of the accessibility subindex remained relatively stable throughout the study period.

Table 1
Descriptive statistics of 13 indicators of the bikeability index (N=57080).

Index	Indicators	Maximum	Minimum	Mean	Standard deviation
Safety	Wind speed (m s^{-1})	7.78	1.35	5.02	1.83
	Slope	25.57	0.00	3.68	2.50
	Precipitation (mm)	0.01	0	0.002	0.004
Comfort	Temperature (°C)	20.74	15.73	17.95	1.19
	Sky view index	0.64	0.00	0.16	0.15
	Green view index	0.48	0.00	0.05	0.09
	Sinuosity	0.98	0.00	0.26	0.19
	PM2.5 (μg m^{-3})	32.36	9.18	18.13	8.48
Accessibility	Average speed (m s^{-1})	49.51	0.00	7.33	4.48
	Public transport	4,128.33	0.05	330.41	403.44
	Commercial	149	0.00	7.13	10.87
Vitality	Number of trajectories	2,230	0.00	26.59	50.54
	Crowdedness	21,941	0.00	4,146	2,994.18

Table 2
Weighted coefficients of 13 indicators of the bikeability index.

Variables	Indicators	Weighted coefficients
x_1	Wind speed (m s^{-1})	0.097
x_2	Slope	0.149
x_3	Precipitation (mm)	−0.102
x_4	Temperature (°C)	0.128
x_5	Sky view index	0.038
x_6	Green view index	0.138
x_7	Sinuosity	0.073
x_8	PM2.5 (μg m^{-3})	−0.069
x_9	Average speed (m s^{-1})	0.104
x_{10}	Public transport	0.124
x_{11}	Commercial	0.075
x_{12}	Number of trajectories	0.168
x_{13}	Crowdedness	0.077

The vitality subindex is demonstrated in the last row of Fig. 4. Unlike the safety and comfort subindexes, it only shows a notable fluctuation on one day, the 23rd, with a decrease to 0.013. On all the other days, the value of the vitality subindex remained constant at 0.015. This stability is likely due to consistent commuting patterns on weekdays. However, on the 23rd, the rainy weather caused a reduction in the number of cycling trips from 300,000 to 120,000, resulting in a decrease in the vitality subindex.

4.2. Spatial and temporal analysis of the bikeability index

The calculation of the bikeability index requires assigning appropriate weights to each indicators. To determine these weights, we performed a principal component analysis (PCA) on the 13 indicators. The PCA resulted in 6 components, providing a balance between a minimal number of components and reliable explained variance. The relationships between components and indicators are displayed in Fig. 5. The final weighted coefficients for calculating the bikeability index using the weighted indicators are derived as follows 2.

As per the method outlined above, the bikeability index for the study area and period has been generated. It is a dynamic index that takes into account both the spatial and temporal aspects, with road segments as its spatial unit and minutes as its temporal unit. Fig. 6 provides an illustration of the dynamic trend of the bikeability index. Fig. 6(a) displays a map of the index (number of trajectories) on the 24th, between 6:00 a.m. and 9:00 a.m. Fig. 6(b) showcases the time series of the bikeability index in relation to the number of shared bicycle tracks on Hubin Road.

The spatial distribution of the bikeability index is shown in Fig. 7, which presents an averaged value map of Xiamen Island. The regions with high bikeability index values are mainly located around Hubin Nanlu and Hubin Beilu, which serve as key roads for public transportation and are home to numerous bus stations. Furthermore, these areas are surrounded by a variety of commercial and residential communities. This results in a high accessibility subindex as well as high levels of crowdedness, contributing to a high value of the vitality subindex. The combination of these high subindexes values ultimately results in a high overall bikeability index in this region.

The temporal distribution of the bikeability index shows a fluctuation throughout the study period, as seen in Fig. 8. On the 21st and 22nd, the average values were recorded as 0.236 and 0.233, respectively. On the 23rd, however, there was a noticeable drop in the bikeability index value, reaching a low of 0.098. Despite this decrease, the values rebounded to 0.188 and 0.185 on the 24th and 25th, respectively. This fluctuation in the bikeability index is mainly due to a rainfall event that occurred in Xiamen on the 23rd. The rainy conditions led to a significant decrease in the safety subindex, which in turn decreased the overall value of the bikeability index.

The hourly pattern of the bikeability index reveals a different trend compared to the daily change (Fig. 8). As seen in Fig. 8, the hourly bikeability index values exhibit much less fluctuation. The value was recorded as 0.184 at 6:00 a.m. and then gradually increased, reaching its peak at 7:00 a.m. and 8:00 a.m. with values of 0.198 and 0.195, respectively. This increase was mainly due to an increase in the vitality subindex, as more people were using shared bicycles between 7:00 a.m. and 8:00 a.m. on working days. However, at 9:00 a.m., the value dropped to its lowest point at 0.17.

4.3. Hotspot area validation

To validate the bikeability index, we analyzed the spatiotemporal patterns of shared bicycle cycling trajectories to determine if they align with general expectations. Our approach included a hotspot analysis of 15-minute intervals of data from the 21st, using a grid with a 165 × 165 m spatial resolution (Fig. 9). The area surrounding Xiamen Island was a continuous cold spot, indicating low levels of cycling activity in the morning. The northern and eastern areas of the island were oscillating cold spots, indicating low levels of cycling activity during the morning but turned into hop spots during rush hour when traffic demand is high. The central and eastern part of the island was an oscillating hot spot, showing high levels of cycling activity throughout most of the morning, with a few exceptions at 6:00 a.m. or 10:00 a.m. Surrounded by oscillating hot spots, three consecutive hot spots had a high level of cycling activity throughout the morning.

To further validate our proposed index, we conducted a case study analysis in the central area of Xiamen CR, which is the middle continuous hotspot area. The location of this case study is the shared bicycle cycling hotspot at the intersection of Hubin Nanlu and Hubin Donglu, near the commercial center of Xiamen Wanxiangcheng, between 8:00–9:00 a.m. on December 21, 2020, as shown in Fig. 10.

The study area is centered around the Huarun commercial center, surrounded by a large residential area. During the morning hours, a substantial amount of shared bicycles are used in this region, contributing to a relatively high bikeability index. This highlights the significance of cycling routes in determining the level of bikeability.

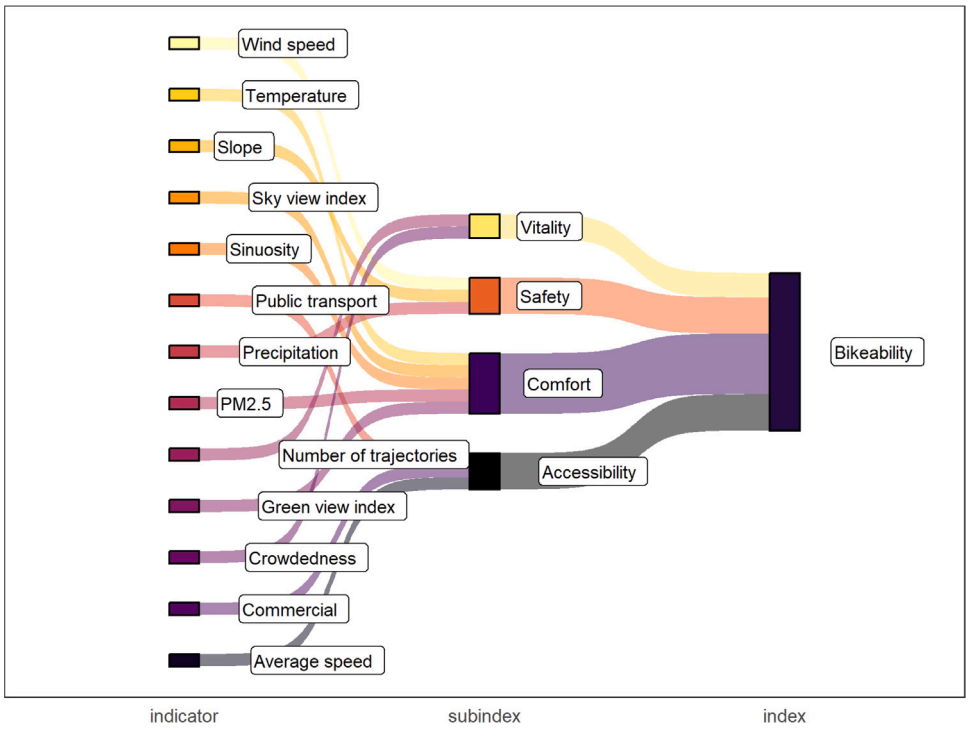

Fig. 5. The PCA result for 13 indicators indicates correspondence between principal components and original indicators.

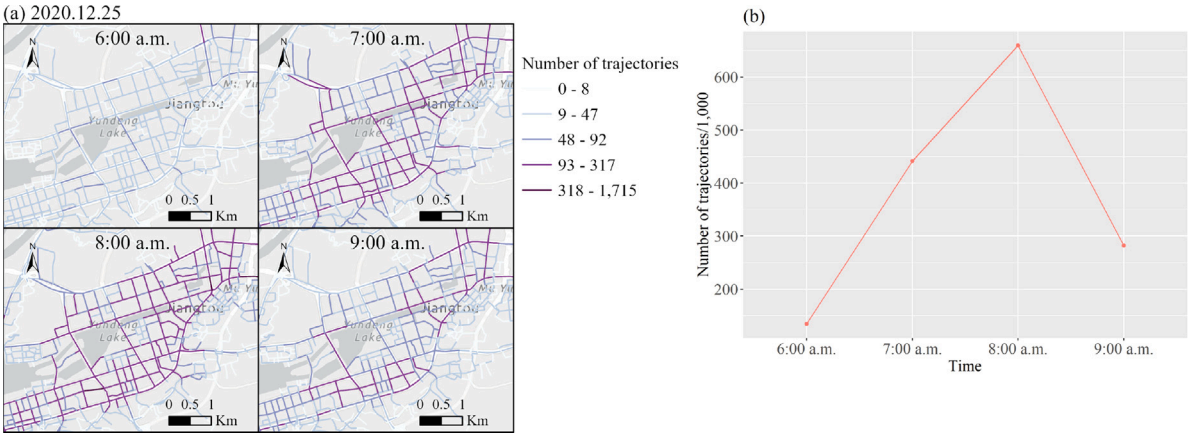

Fig. 6. (a) Number of trajectories of Xiamen on the 25th at 6:00, 7:00, 8:00, and 9:00 a.m., (b) different time periods of the number of shared bicycle tracks.

The current cycling infrastructure falls short of supporting high-friendly cycling routes. For example, the road section near Hubin Middle School, which is located in a residential area and has a high demand for commuting, features a high density of shared bicycle stops, catering, shopping, and life services. The natural environment also favors cycling with low slopes, moderate wind speed, low precipitation, suitable temperature, overcast weather, and good air quality. Despite these favorable conditions, this section is congested during the morning rush hour due to a narrow non-motorized lane, slow average speed, and high volume of people commuting and going to school, resulting in low bikeability in this section despite high cycling activity.

Furthermore, the demand for shared bicycles in hot spot regions is much higher, underscoring the importance of ensuring the availability of bicycles and easy accessibility. As shown in the figure, most road sections in the hot spot area have high densities of parking spots. However, there is a shortage of parking spots on the east side of Huarun Center, leading to a concentration of cyclists in other areas, causing congestion and potentially affecting commuting efficiency.

This case study showcases how our bikeability index takes into account the purpose of cycling and reflects cyclists' preferred routes. Nonetheless, there remain disparities between the actual infrastructure, preferred routes, and regional conditions. By integrating the index system with real-time data, it is possible to provide suggestions for enhancing regional cycling conditions. The findings of this research can guide management departments and shared bicycle providers to improve facilities and offer optimal route planning for cyclists to avoid congestion and overcome difficulties in finding available bicycles. In conclusion, the bikeability index can provide comprehensive decision-making recommendations and advance the development of cycling-friendly cities.

5. Discussion

In the following section, we delve into the advantages, consequences, and practical implications of our framework and its product. We conclude by highlighting the potential of our framework to advance sustainability in urban planning and transportation management.

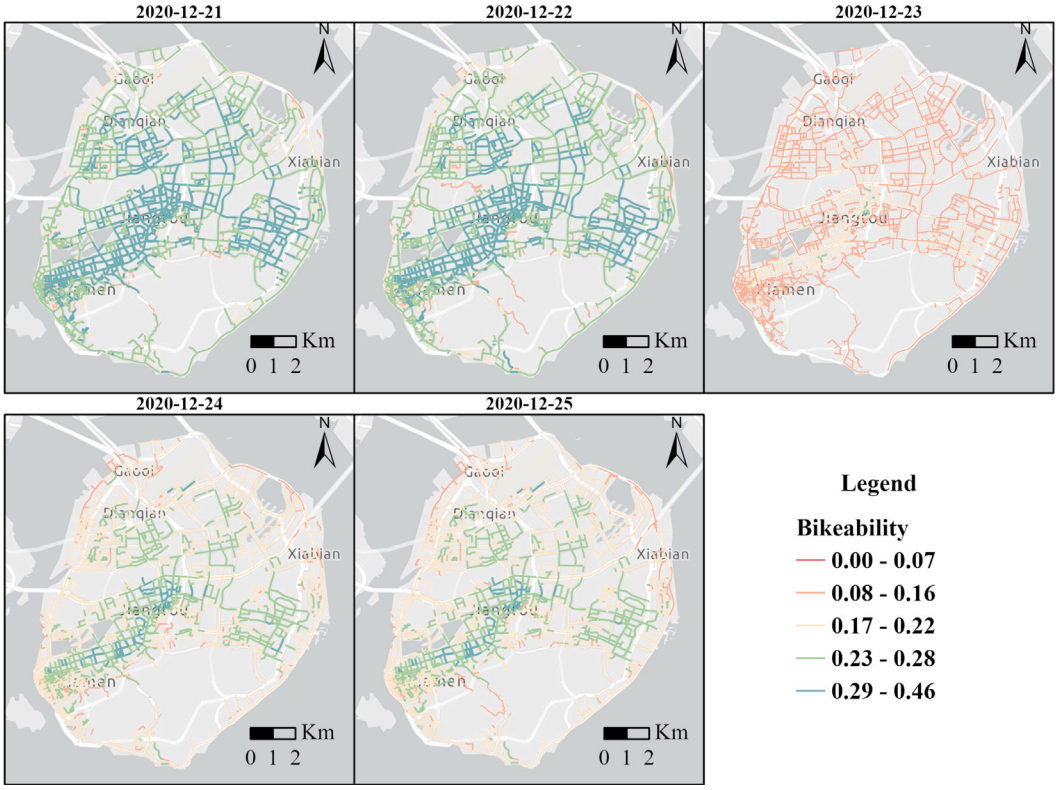

Fig. 7. Average bikeability of Xiamen Island on December 21th, 22th, 23th, 24th, 25th, 2020, the roads highlighted in red indicate lower levels of bikeability, whereas those in green indicate higher levels of bikeability. (For interpretation of the references to color in this figure legend, the reader is referred to the web version of this article.)

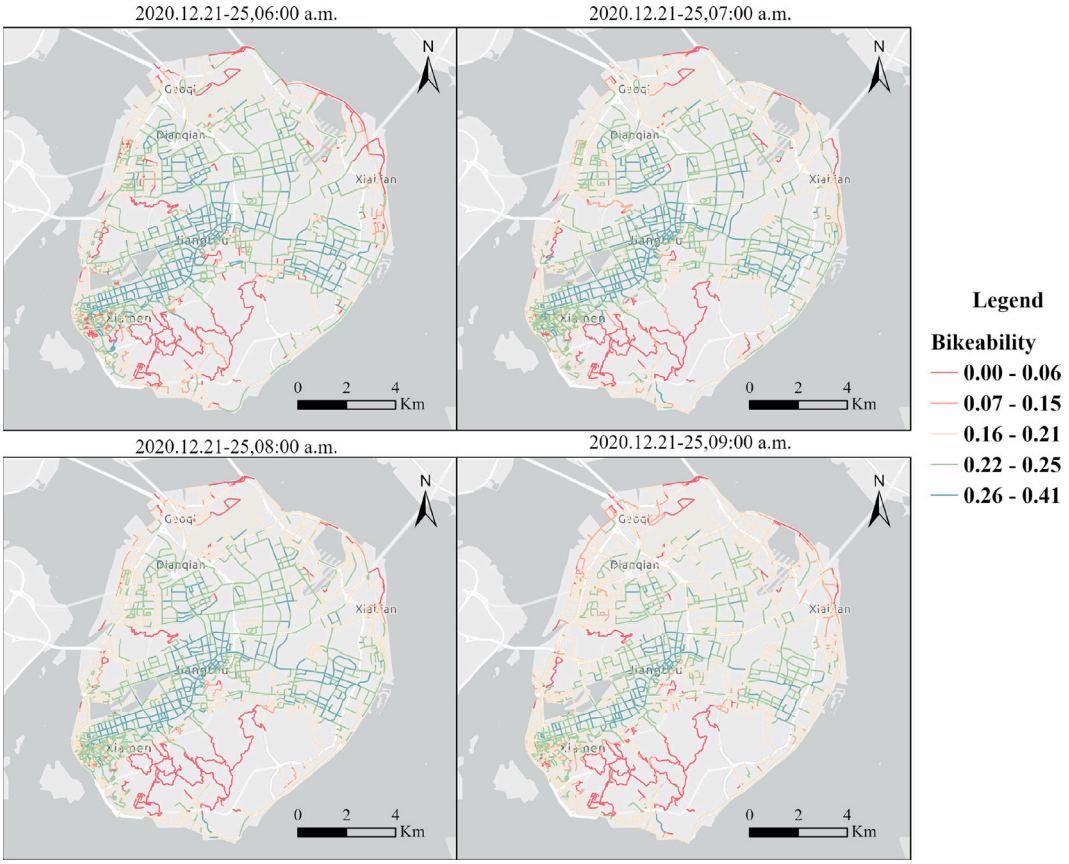

Fig. 8. Average bikeability of Xiamen Island at 6:00, 7:00, 8:00, and 9:00 a.m., the roads highlighted in red indicate lower levels of bikeability, whereas those in green indicate higher levels of bikeability. (For interpretation of the references to color in this figure legend, the reader is referred to the web version of this article.)

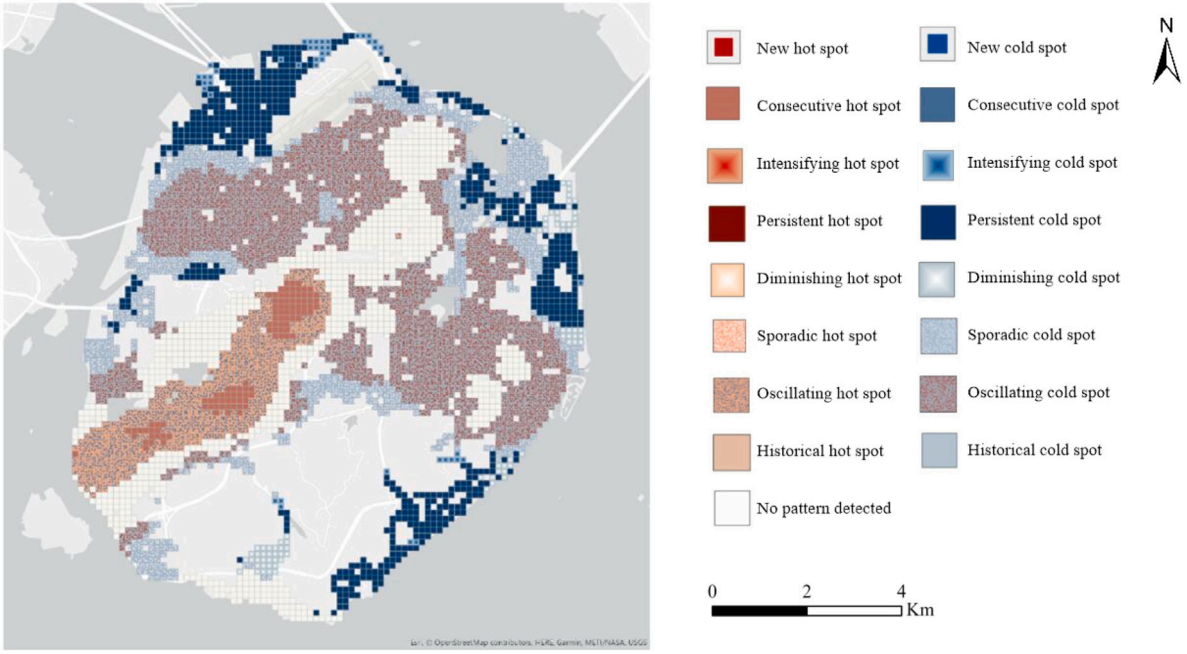

Fig. 9. Spatiotemporal hotspot analysis of Xiamen Island.

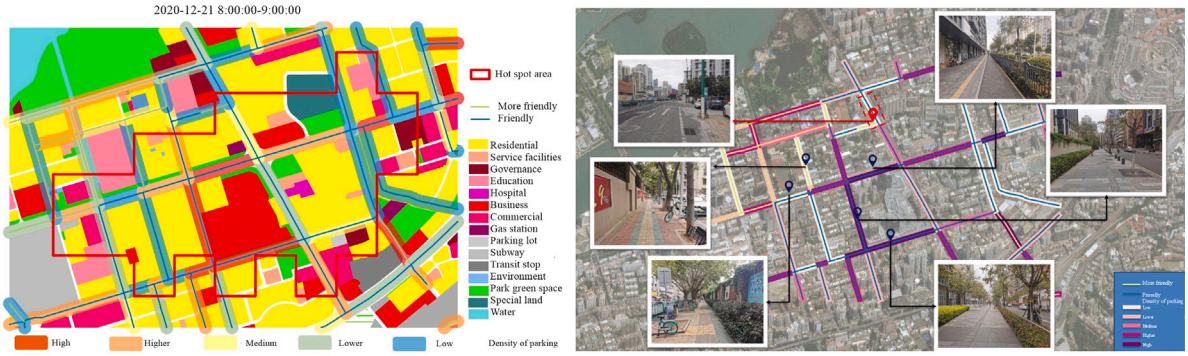

Fig. 10. Case study field validation.

5.1. Influence of indicators

- **Natural environmental factors**: Natural environmental factors play a crucial role in determining cycling friendliness, and although their spatial distribution did not vary significantly, the temporal distribution had a significant impact. Analysis of the day-to-day distribution of cycling friendliness revealed that even in the absence of extreme weather events, weather conditions affected cycling friendliness. For instance, on December 23, the average ride friendliness value was lower compared to other dates, attributed to rainfall.
- **Built environment factors**: Built environment factors, including commercial accessibility, public transportation accessibility, and the distribution of jobs and residences, also play a significant role in determining commuter friendliness. In this study, despite the smooth road and gentle slope of the traffic circle, the sparse distribution of commercial facilities, long distance of public transportation stops, and a small number of jobs and residences led to lower cycling activity during the morning peak period, which was identified as less friendly in the evaluation model.

5.2. Innovation and limitations

- **Fusion of multi-source geospatial big data**: The fusion of multi-source geospatial big data enables a more comprehensive evaluation of cycling friendliness. This includes the analysis of spatio-temporal data from sources such as street view imagery, POI, DEM, and air quality. The use of dynamic cycling trajectories provides insight into the path choices of residents, which improves the problem of sampling bias and allows for multi-source data fusion research. However, the time registration of multi-source data may not be entirely consistent and may not represent the entire research area accurately. Therefore, future studies should consider employing field observations and alternative data sources to validate the findings of this study (Jia et al., 2019).
- **Refinement of research methods and scales**: This study employs a combination of GIS spatial analysis, statistical analysis, deep learning techniques, and trajectory mining algorithms, which can effectively integrate various types of multi-source data and enhance the depth and breadth of research insights. The study provides an extensive analysis of the road network, offering an intuitive visual representation of the cycling-friendliness of urban

roads. This approach enhances the scalability of the study, enabling a more comprehensive analysis of the cycling friendliness of urban areas.

While this study provides valuable insights into the evaluation of bikeability, there are several limitations to consider. First, the conceptualization of "bikeability" as a distinct metric bridging the built environment and cycling behavior is not universally established in academia. It is worth noting that Codina et al. Fosgerau et al. and Reggiani et al. offer varied definitions (Codina et al., 2022; Fosgerau et al., 2023; Reggiani et al., 2022). Considering such discrepancies, we adopted an empirically derived definition. Here, "bikeability" encompasses four sub-indices and thirteen indicators, all of which were meticulously gauged and validated within the context of our local study area, leveraging multi-source geospatial data. While this index is aptly tailored for various practical contexts, we recognize its intrinsic constraints in fully encompassing the breadth of bikeability assessment. Second, the study does not yet examine the inter-correlation among individual indicators. It requires further research to fully understand the individual contribution of each subindex to a comprehensive conceptualization of bikeability. Bikeability as defined by the weighted coefficients obtained from a PCA provides a comprehensive and objective way to relate the different factors (Bao et al., 2022; Liu et al., 2022). Third, we realize that the study so far does not fully delve into the contribution of each specific indicator to the characteristics of the spatial and temporal distribution. We plan to address this issue in future studies. Fourth, we acknowledge that certain indicators employed in our bikeability assessment are not entirely accessible. Notably, indicators that merge cycling-related data with population trends could offer significant insights. In subsequent research, we intend to incorporate broader and more readily accessible indicators, while also delving deeper into the impact of specific indicators on intervention strategies. Possible ways to do so could be to use different weighing algorithms including, AHP, Delphi, DEA, machine learning, and deep learning and to consider a hierarchical setting of weights (Gdoura et al., 2015; Xie et al., 2017; Hong and Mwakalonge, 2020; Ki et al., 2023). This should then result in policy recommendations also for other cities.

5.3. Implications for policy and practice

The variability in the bikeability index across different segments presents an opportunity for transportation planners to enhance cycling infrastructure. Monitoring the spatiotemporal dynamics of bikeability can help identify potential environmental or infrastructure changes and their impact on the community's level of bikeability. To ensure the relevance of the cycling friendliness index, case studies that incorporate additional infrastructure data are necessary for local comparison of bikeability results, enabling the proposal of landable solutions for varying infrastructure. For instance, the fusion analysis of parking spot electronic fence data and bikeability could expose discrepancies between regional cycling infrastructure and cyclists' preferences, providing actionable recommendations to government departments and guiding users to cycle in a more bike-friendly manner.

6. Conclusion

We have developed a new framework for quantifying bikeability that considers dynamic environmental factors, which were previously overlooked in existing research. The proposed framework comprises four sub-indices: safety, comfort, accessibility, and vitality, and employs open-source data, advanced deep neural network and GIS spatial analysis, which eliminate subjective evaluations and are less time-consuming than prior methods. The resulting comprehensive spatiotemporal assessment of the bikeability/cycling index can facilitate the construction of sustainable cycling infrastructure.

We used Xiamen as a case study to validate our approach. Our study's outcomes demonstrate that Xiahe-South Hubin Road, Software Industrial Parks, Huli Innovation Parks, and Lujiang Business District in Xiamen's central business district are more bike-friendly, as evidenced by their elevated safety, accessibility, and vitality, resulting in higher bikeability scores. Nonetheless, traffic congestion, which lowers cycling speed and actual bikeability, is a potential downside of the higher vitality levels. To enhance cycling mobility, air quality, green spaces, and public transportation facilities need to be enhanced in areas with lower bikeability scores.

Our novel bikeability framework employs readily comprehensive spatially-detailed data, making it easily implementable on a broad scale. Urban planners, transportation policymakers, and environmental decision-makers can objectively assess bikeability and design comprehensive cycling infrastructure using the developed bikeability index.

Declaration of competing interest

The authors declare that they have no known competing financial interests or personal relationships that could have appeared to influence the work reported in this paper.

Data availability

The authors do not have permission to share data.

Acknowledgement

This study was supported by the National Natural Science Foundation of China (42271433), the Fundamental Research Funds for the Central Universities (2042023kfyq04), Jiangxi Provincial 03 Special Foundation and 5G Program (20224ABC03A05), Wuhan University Specific Fund for Major School-level Internationalization Initiatives (WHU-GJZDZX-PT07), and the International Institute of Spatial Lifecourse Health. We also thank the Digital China Innovation Contest 2021 and Xiamen Urban Planning and Design Institute for their help in data collection. Shaoqing Dai is funded by the Chinese Scholarship Council (201904910428).

References

Bao, Z., Shifaw, E., Deng, C., Sha, J., Li, X., Hanchiso, T., Yang, W., 2022. Remote sensing-based assessment of ecosystem health by optimizing vigor-organization-resilience model: A case study in Fuzhou City, China. Ecol. Inform. 72, 101889.

Caigang, Z., Shaoying, L., Zhangzhi, T., Feng, G., Zhifeng, W., 2022. Nonlinear and threshold effects of traffic condition and built environment on dockless bike sharing at street level. J. Transp. Geogr. 102, 103375.

Chen, Y., Zhang, Y., Coffman, D., Mi, Z., 2022. An environmental benefit analysis of bike sharing in New York City. Cities 121, 103475.

Chen, L.C., Zhu, Y., Papandreou, G., Schroff, F., Adam, H., 2018. Encoder-decoder with atrous separable convolution for semantic image segmentation. In: Proceedings of the European Conference on Computer Vision. ECCV, pp. 801–818.

Codina, O., Maciejewska, M., Nadal, J., Marquet, O., 2022. Built environment bikeability as a predictor of cycling frequency: Lessons from Barcelona. Transp. Res. Interdiscip. Perspect. 16, 100725.

Dai, S., Ren, Y., Zuo, S., Lai, C., Li, J., Xie, S., Chen, B., 2020. Investigating the uncertainties propagation analysis of CO2 emissions gridded maps at the urban scale: A case study of Jinjiang City, China. Remote Sens. 12 (23), 3932.

Eren, E., Uz, V.E., 2020. A review on bike-sharing: The factors affecting bike-sharing demand. Sustain. Cities Soc. 54, 101882.

Fosgerau, M., Łukawska, M., Paulsen, M., Rasmussen, T.K., 2023. Bikeability and the induced demand for cycling. Proc. Natl. Acad. Sci. 120 (16), e2220515120.

Gan, Z., Yang, M., Zeng, Q., Timmermans, H.J., 2021. Associations between built environment, perceived walkability/bikeability and metro transfer patterns. Transp. Res. A 153, 171–187.

Gdoura, K., Anane, M., Jellali, S., 2015. Geospatial and AHP-multicriteria analyses to locate and rank suitable sites for groundwater recharge with reclaimed water. Resour. Conserv. Recy. 104, 19–30. http://dx.doi.org/10.1016/j.resconrec.2015.09.003.

Giallouros, G., Kouis, P., Papatheodorou, S.I., Woodcock, J., Tainio, M., 2020. The long-term impact of restricting cycling and walking during high air pollution days on all-cause mortality: Health impact Assessment study. Environ. Int. 140, 105679.
Hagen, O.H., Rynning, M.K., 2021. Promoting cycling through urban planning and development: a qualitative assessment of bikeability. Urban Plan. Transp. Res. 9 (1), 276–305.
Hankey, S., Lindsey, G., Marshall, J.D., 2017. Population-level exposure to particulate air pollution during active travel: Planning for low-exposure, health-promoting cities. Environ. Health Perspect. 125, 527–534.
Hong, J.D., Mwakalonge, J.L., 2020. Biofuel logistics network scheme design with combined data envelopment analysis approach. Energy 209, 118342. http://dx.doi.org/10.1016/j.energy.2020.118342.
Huang, X., Li, Z., Jiang, Y., Ye, X., Deng, C., Zhang, J., Li, X., 2021. The characteristics of multi-source mobility datasets and how they reveal the luxury nature of social distancing in the US during the COVID-19 pandemic. Int. J. Digit. Earth 14 (4), 424–442.
Huang, X., Martin, Y., Wang, S., Zhang, M., Gong, X., Ge, Y., Li, Z., 2022a. The promise of excess mobility analysis: measuring episodic-mobility with geotagged social media data. Cartogr. Geogr. Inf. Sci. 49 (5), 464–478.
Huang, X., Wang, S., Zhang, M., Hu, T., Hohl, A., She, B., Gong, X., Li, J., Liu, X., Gruebner, O., et al., 2022b. Social media mining under the COVID-19 context: Progress, challenges, and opportunities. Int. J. Appl. Earth Obs. Geoinf. 113, 102967.
Hyland, M., Frei, C., Frei, A., Mahmassani, H.S., 2018. Riders on the storm: Exploring weather and seasonality effects on commute mode choice in Chicago. Travel Behav. Soc. 13, 44–60.
Ito, K., Biljecki, F., 2021. Assessing bikeability with street view imagery and computer vision. Transp. Res. C 132, 103371.
Jia, P., 2021. Obesogenic environment and childhood obesity. Obes. Rev. 22, e13158.
Jia, P., Cao, X., Yang, H., Dai, S., He, P., Huang, G., Wu, T., Wang, Y., 2021. Green space access in the neighbourhood and childhood obesity. Obes. Rev. 22, e13100.
Jia, P., Cheng, X., Xue, H., Wang, Y., 2017. Applications of geographic information systems (GIS) data and methods in obesity-related research. Obes. Rev. 18 (4), 400–411.
Jia, P., Xue, H., Liu, S., Wang, H., Yang, L., Hesketh, T., Ma, L., Cai, H., Liu, X., Wang, Y., 2019. Opportunities and challenges of using big data for global health. Sci. Bull. 64 (22), 1652–1654.
Kellstedt, D.K., Spengler, J.O., Foster, M., Lee, C., Maddock, J.E., 2021. A scoping review of bikeability assessment methods. J. Community Health 46, 211–224.
Ki, D., Chen, Z., Lee, S., Lieu, S., 2023. A novel walkability index using google street view and deep learning. Sustainable Cities Soc. 99, 104896. http://dx.doi.org/10.1016/j.scs.2023.104896.
Lemke, C., Bastini, K., 2020. Embracing multiple perspectives of sustainable development in a composite measure: The Multilevel Sustainable Development Index. J. Clean. Prod. 246, 118884.
Liu, L., Zhao, G., An, Z., Mu, X., Jiao, J., An, S., Tian, P., 2022. Effect of grazing intensity on alpine meadow soil quality in the eastern Qinghai-Tibet Plateau, China. Ecol. Indic. 141, 109111.
Long, Y., Zhao, J., 2020. What makes a city bikeable? a study of intercity and intracity patterns of bicycle ridership using mobike big data records. Built Environ. 46 (1), 55–75.
Lowry, M.B., Callister, D., Gresham, M., Moore, B., 2012. Assessment of communitywide bikeability with bicycle level of service. Transp. Res. Rec. 2314 (1), 41–48.
Nielsen, T.A.S., Skov-Petersen, H., 2018. Bikeability – Urban structures supporting cycling. Effects of local, urban and regional scale urban form factors on cycling from home and workplace locations in Denmark. J. Transp. Geogr. 69, 36–44.
Pan, X., Zhao, L., Luo, J., Li, Y., Zhang, L., Wu, T., Smith, M., Dai, S., Jia, P., 2021. Access to bike lanes and childhood obesity: a systematic review and meta-analysis. Obes. Rev. 22, e13042.
Parkin, J., Wardman, M., Page, M., 2007. Models of perceived cycling risk and route acceptability. Accid. Anal. Prev. 39 (2), 364–371.
Porter, A.K., Kohl, H.W., Pérez, A., Reininger, B., Pettee Gabriel, K., Salvo, D., 2020. Bikeability: Assessing the objectively measured environment in relation to recreation and transportation bicycling. Environ. Behav. 52, 861–894.
Ran, L., Tan, X., Xu, Y., Zhang, K., Chen, X., Zhang, Y., Li, M., Zhang, Y., 2021. The application of subjective and objective method in the evaluation of healthy cities: A case study in Central China. Sustainable Cities Soc. 65, 102581.
Reggiani, G., Van Oijen, T., Hamedmoghadam, H., Daamen, W., Vu, H.L., Hoogendoorn, S., 2022. Understanding bikeability: a methodology to assess urban networks. Transportation 49 (3), 897–925.
Steinacker, C., Storch, D.M., Timme, M., Schröder, M., 2022. Demand-driven design of bicycle infrastructure networks for improved urban bikeability. Nat. Comput. Sci. 2 (10), 655–664.
Tang, Y., Song, S., Gui, S., Chao, W., Cheng, C., Qin, R., 2023. Active and low-cost hyperspectral imaging for the spectral analysis of a low-light environment. Sensors 23 (3), 1437.
Tran, P.T.M., Zhao, M., Yamamoto, K., Minet, L., Nguyen, T., Balasubramanian, R., 2020. Cyclists' personal exposure to traffic-related air pollution and its influence on bikeability. Transp. Res. D 88, 102563.
Wang, K., Akar, G., Chen, Y.J., 2018. Bike sharing differences among millennials, gen xers, and baby boomers: Lessons learnt from new york city's bike share. Transp. Res. A 116, 1–14.
Wang, M., Chen, Z., Rong, H.H., Mu, L., Zhu, P., Shi, Z., 2022. Ridesharing accessibility from the human eye: Spatial modeling of built environment with street-level images. Comput. Environ. Urban Syst. 97, 101858.
Winters, M., Brauer, M., Setton, E.M., Teschke, K., 2010. Built environment influences on healthy transportation choices: bicycling versus driving. J. Urban Health 87, 969–993.
Wold, S., Esbensen, K., Geladi, P., 1987. Principal component analysis. Chimometrics and intelligent laboratory systems. In: IEEE Conference on Emerging Technologies & Factory Automation Efta. pp. 704–706.
Xie, J., Chen, W., Zhang, D., Zu, S., Chen, Y., 2017. Application of principal component analysis in weighted stacking of seismic data. IEEE Geosci. Remote Sens. Lett. 14 (8), 1213–1217. http://dx.doi.org/10.1109/LGRS.2017.2703611.
Yang, S., Chen, X., Wang, L., Wu, T., Fei, T., Xiao, Q., Zhang, G., Ning, Y., Jia, P., 2021. Walkability indices and childhood obesity: a review of epidemiologic evidence. Obes. Rev. 22, e13096.
Yu, G., Yu, Q., Hu, L., Zhang, S., Fu, T., Zhou, X., He, X., Liu, Y., Wang, S., Jia, H., 2013. Ecosystem health assessment based on analysis of a land use database. Appl. Geogr. 44, 154–164.
Zhang, F., Fan, Z., Kang, Y., Hu, Y., Ratti, C., 2021. "Perception bias": Deciphering a mismatch between urban crime and perception of safety. Landsc. Urban Plan. 207, 104003.
Zhang, F., Wu, L., Zhu, D., Liu, Y., 2019. Social sensing from street-level imagery: A case study in learning spatio-temporal urban mobility patterns. ISPRS J. Photogramm. Remote Sens. 153, 48–58.
Zhao, P., Li, S., Li, P., Liu, J., Long, K., 2018. How does air pollution influence cycling behaviour? Evidence from Beijing. Transp. Res. D 63, 826–838.
Zhao, W., Persello, C., Stein, A., 2022. Extracting planar roof structures from very high resolution images using graph neural networks. ISPRS J. Photogramm. Remote Sens. 187, 34–45.
Zhao, W., Persello, C., Stein, A., 2023. Semantic-aware unsupervised domain adaptation for height estimation from single-view aerial images. ISPRS J. Photogramm. Remote Sens. 196, 372–385.
Zhu, X.X., Wang, Y., Kochupillai, M., Werner, M., Häberle, M., Hoffmann, E.J., Taubenböck, H., Tuia, D., Levering, A., Jacobs, N., et al., 2022. Geo-information harvesting from social media data. arXiv preprint arXiv:2211.00543.